



On the Inclination of a Flying Buttress Arch

Albert Samper¹ · Rodrigo Martín-Sáiz¹ · Blas Herrera²

Accepted: 24 May 2022

© The Author(s) 2022, corrected publication 2022

Abstract

Historically in architecture, the inclination of a flying buttress arch is determined as the amplitude of the angle that spans between the horizontal straight line and the straight line connecting the two ends of the arch's lower edge. Nonetheless, this inclination does not represent the entire flyer, but at most only its lower edge. Therefore, using techniques based on geometrical and mechanical criteria, applied to twenty flyer arches belonging to twelve flying buttresses from several European Gothic cathedrals, we present a new proposal for a definition of inclination which represents the entire arch.

Keywords Flying buttress · Flyer arches · Inclination · Geometric regression · Gothic cathedrals

Introduction

Many authors have carried out research on the origin of flying buttresses (see, for instance, Lefevre-Pontalis 1919; Prache 1976; Henriet 1978, 1982; Stanley 2006). We wish to highlight the work by Viollet-Le-Duc (1996) and Choisy (1899), who theorized the use of the first flying buttresses to strengthen the structure of Vézelay Abbey, which was built in the year 1138. Both authors pointed out that, over the years, the abbey's structure experienced a progressive deformation due to the height of the central nave vaults. They formulated similar hypotheses about the actions taken by the builders in order to counter the thrusts of the central nave and avoid

✉ Blas Herrera
blas.herrera@urv.cat

Albert Samper
albert.samper@urv.cat

Rodrigo Martín-Sáiz
rodrigo.martin@urv.cat

¹ Escola Tècnica Superior d'Arquitectura, Universitat Rovira i Virgili, Reus, Spain

² Departament d'Enginyeria Informàtica i Matemàtiques, Universitat Rovira i Virgili, Avinguda Països Catalans, 26, 43007 Tarragona, Spain

the collapse of the building. Both authors concluded that the builders of that time must have strengthened and supported the structure by means of inclined stone arches, even though Choisy (1899: 300–301) stated that these support elements were initially inclined wooden struts.

These inclined struts successfully countered the horizontal thrusts and relieved stress. Flying buttresses—or stone struts, as Blas Orive (2019) calls them—are the structural elements which fulfil this role in Gothic cathedrals.

Historically, the inclination of a flying buttress arch is determined as the amplitude of the angle that spans between the horizontal straight line and the straight line connecting the two ends of the arch's lower edge (Nikolinakou et al. 2005). This method originally resembles the method used to determine a straight strut's inclination, namely the angle defined by the horizontal straight line with the strut's axis. We believe that such definition of a flying buttress arch inclination (i.e., flyer inclination) is not adequate because of three problems:

- The determination of two endpoints from the lower edge of a flyer arch is an arbitrary and subjective procedure, and the resulting angle value may vary depending on this choice (Fig. 1).
- The deterioration due to the passing of time, seismic disturbances, structural deformations and other incidents of diverse nature may alter the geometric nature and the original shape of the flyer's edge contour, so that the angle value obtained has even less geometric meaning.
- The inclination value for the entire flyer should not be determined on the basis of its lower edge only. Besides, this edge sometimes features ornaments, making this angle even less representative of the entire flyer's inclination.

As will be noted throughout this paper, the first two problems may have an objective solution by means of geometry (using geometric regression), but the third problem cannot be solved, since an inclination value as determined from the lower edge only is not representative of the entire flyer. It is particularly for this reason that this paper presents a new proposal for a definition of a flyer inclination, using

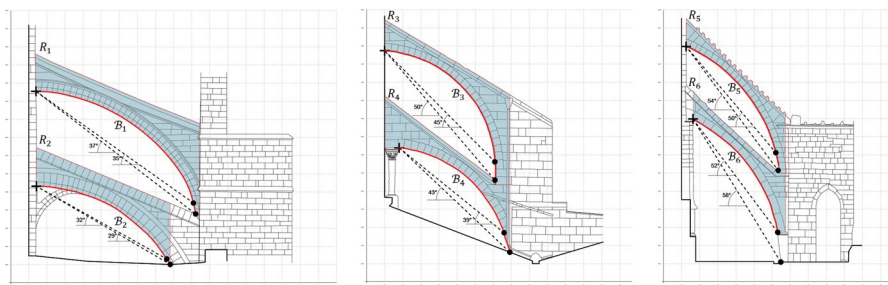


Fig. 1 Some examples of determination of the inclination of several flyers from the cathedrals in Mallorca, Burgos and León using the classical (subjective) criterion. The lower edges B_{1-2} , B_{3-4} and B_{5-6} of the flyers from Mallorca, Burgos and León, respectively, are shown in red. The regions R_{1-2} , R_{3-4} and R_{5-6} of the flyers are highlighted in grey

graphic static analysis techniques to take into account the shape of the entire flyer, not only its lower edge, and its mechanical behaviour.

This new proposal has been applied to twenty flyers belonging to twelve Gothic cathedrals from three European countries: Mallorca, Burgos, León, Oviedo and Toledo, in Spain; Chartres, Saint Pierre in Chartres, Amiens and Saint Denis, in France; and Salisbury, Wells and Bath, in England (Fig. 2).

Methods

“Objective Procedure to Determine the Inclination of a Flying Buttress Arch Under the Classical Criterion” presents a circular regression procedure which provides an objective solution to problem (a), regarding the arbitrariness involved in choosing two end points of the lower edge of a flyer in order to determine the flyer’s inclination according to the classical criterion (Fig. 1). As will be made clear in “Objective Procedure to Determine the Inclination of a Flying Buttress Arch Under the Classical Criterion”, this procedure allows for the determination of the flyer’s inclination even if several agents may have altered the shape and the geometric nature of the flyer’s edge. Therefore, it solves problem (b) as well.

Despite providing a geometric procedure to determine the inclination of a flyer according to the classical criterion, we point out again that this parameter does not represent the entire structural element, but is only related to its lower edge. Claiming that the resulting angle is the inclination of the entire flyer is conceptually disproportionate. This is why in “Objective Procedure to Determine the Inclination of a Flying Buttress Arch Using Mechanical Criteria and Graphic Statics Techniques” we present a new definition of inclination and a new procedure which makes use of graphic statics techniques and concepts, and takes into account the entire flyer and its structural function.

These procedures have been applied to twenty flyers from several European cathedrals. After visiting the twelve sites and taking photographs of all flying buttress details, we carried out a topographic reconstruction using photogrammetric techniques and the Agisoft PhotoScan Professional software product (Figs. 3, 4).

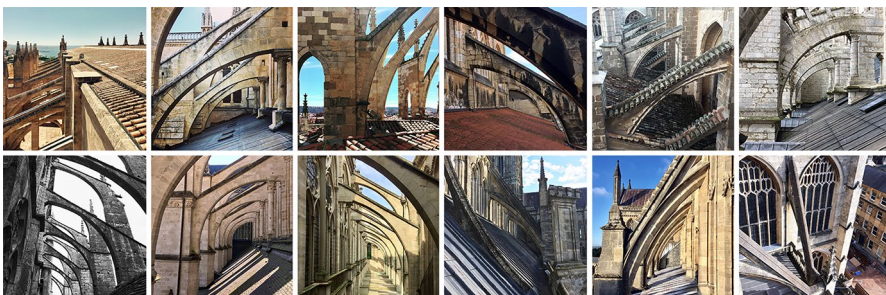


Fig. 2 Photos of the flyers considered in our study. Left to right and top to bottom: Mallorca, Burgos, León, Oviedo, Toledo, Chartres, Saint Pierre in Chartres, Amiens, Saint Denis, Salisbury, Wells and Bath

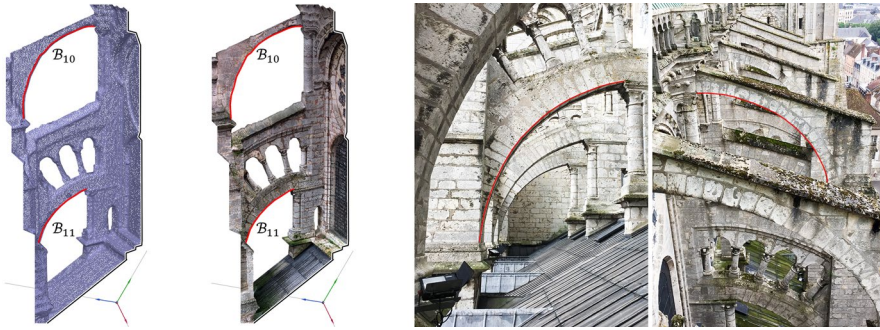


Fig. 3 On the left, two models resulting from the photogrammetric process. On the right, two photographs showing the two flyers of this flying buttress. The lower edges B_{10-11} of these flyers (from Chartres cathedral) are shown in red

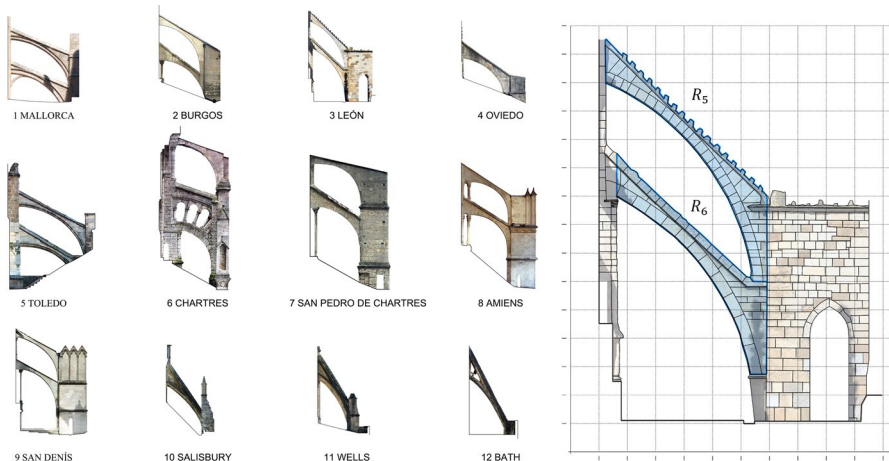


Fig. 4 On the left, twelve models resulting from the photogrammetric process. On the right, an example of a texturized front projection in vector format for the flying buttress from Leon cathedral. The regions R_{5-6} of these two flyers are highlighted in blue

Based on the resulting graphic models, we have obtained a front projection of each element in TIFF format (Fig. 4) which, in turn, has allowed us to draw a linear reconstruction in CAD vector format.

These graphic results provide the following geometric and architectural information:

- A curve outlining the lower edge of each flyer. These edges will be called B_i , where i ranges from 1 to 20. As an example, they are shown in red in Figs. 1 and 3.
- A region which defines each flyer. These regions will be called R_i , where i ranges from 1 to 20. As an example, some of them are highlighted in blue in Figs. 1 and 4.

We chose high quality for all steps of the photogrammetric process in order to obtain a sufficiently dense mesh to map a high-resolution texture. Figure 3 shows a few images from this process, and Table 1 summarizes the data for each generated model. We accepted the default camera calibration parameters provided by the software Photoscan. Besides, for scaling and orientation of each model we introduced at least three markers which generated a mean error of less than 1.5 cm for axes X, Y and Z.

In order to carry out an optimal scaling and vertical levelling of the models, we did as follows: (1) several parts of each flying buttress were measured using a laser distance meter (Leica Disto D2) and, (2) a vertical edge of each flying buttress was identified as the Z-axis of each model using a levelling device. Also, a 1-m long rigid bar was placed beside each flying buttress in order to test the measuring errors in the resulting model.

Objective Procedure to Determine the Inclination of a Flying Buttress Arch Under the Classical Criterion

We find the x,y coordinates ($P_i = (x_i, y_i)$) of 10,000 points P_i which define each of the twenty lower edges \mathcal{B}_{1-20} determined with the abovementioned graphic procedure. This set of 10,000 points is cloud $\mathcal{N}_{1-20} = \{P_i\}_{i=1}^{i=n}$, where $n = 10,000$. With the help of a *lisp* routine called EPC, we obtain a TXT file with the coordinates of the points P_i from the clouds \mathcal{N}_{1-20} , and then we calculate the regression circle γ for each cloud.

In order to calculate the regression circle θ_{1-20} of each cloud \mathcal{N}_{1-20} , we need to find the coefficients of equation $\theta \equiv Bx^2 + By^2 + Ex + Fy + 1 = 0$. This regression circle is the circle which best fits the cloud, minimizing the sum of the quadratic residues $\sum_{i=1}^{i=n} \varepsilon_i^2 = \sum_{i=1}^{i=n} (Bx_i^2 + By_i^2 + Ex_i + Fy_i + 1)^2$. It is widely known that the

Table 1 Data from the meshes for the outer surfaces of the twelve flying buttresses which have been modelled using photogrammetric techniques

No.	Flying buttress from	Number of photos	Number of vertices	Number of faces
1	Mallorca cathedral	67	72,575	140,998
2	Burgos cathedral	76	119,537	198,295
3	León cathedral	56	49,934	96,045
4	Oviedo cathedral	44	91,038	179,999
5	Toledo cathedral	87	95,690	189,170
6	Chartres cathedral	83	78,260	155,225
7	Saint Pierre church in Chartres	40	100,560	215,890
8	Amiens cathedral	67	149,970	296,728
9	Saint Denis cathedral	61	155,567	320,135
10	Salisbury cathedral	61	85,890	168,890
11	Wells cathedral	45	89,987	176,988
12	Bath cathedral	31	49,475	97,489

solution to the problem of calculating the equation θ is given by the Gauss normal equations. Specifically, the following system must be solved:

$$\begin{pmatrix} 1_i(x_i^2 + y_i^2)^2 & x_i(x_i^2 + y_i^2) & y_i(x_i^2 + y_i^2) \\ x_i(x_i^2 + y_i^2) & 1_i x_i^2 & x_i y_i \\ y_i(x_i^2 + y_i^2) & x_i y_i & 1_i y_i^2 \end{pmatrix} \begin{pmatrix} B \\ E \\ F \end{pmatrix} = \begin{pmatrix} -1_i(x_i^2 + y_i^2) \\ -1_i x_i \\ -1_i y_i \end{pmatrix} \quad (1)$$

In this equation, the range of variation for i is $i=1 \div n$ in Einstein summation convention with repeated subscripts, with $1_i = 1$. For example: $x_i y_i = \sum_{i=1}^{i=n} x_i y_i$, and $1_i y_i^2 = \sum_{i=1}^{i=n} y_i^2$. In order to ensure correct results and incorporate them into the CAD software, we have designed our own calculation software.

Readers familiar with the software product Rhinoceros can use the tool “line through points” to determine the regression line of a point cloud.

Figure 6 shows the regression circles of the lower edges \mathcal{B}_j , where j ranges from 1 to 20. Based on these circles, we can determine the center O_j and the radius r_j of each of the twenty flyers belonging to the twelve flying buttresses considered in our paper. Next, we determine angle α_j based on the inclination of the straight line passing through two endpoints. These two endpoints are the points of intersection between the regression circle and the horizontal or vertical straight line passing through the topmost or lowermost point of the considered point cloud \mathcal{N}_j . Figure 5 shows a detailed view of this for some of the flyers considered in this paper.

Table 2, located in Sect. Results of results, shows the value of radius r_j for each regression circle and the angular value α_j of the flyer’s inclination according to the classic criterion. Nonetheless, this angular value of inclination has been objectively determined using the abovementioned circle regression method.

Objective Procedure to Determine the Inclination of a Flying Buttress Arch Using Mechanical Criteria and Graphic Statics Techniques

As already stated in the introduction, the angular value α is only related to the lower edge of the flyer, and it does not represent the entire flyer. To overcome this, we propose a new definition of inclination and a new procedure which makes use of graphic statics techniques and takes into account the entire flyer’s geometry and its function. These techniques are well known and have been widely discussed

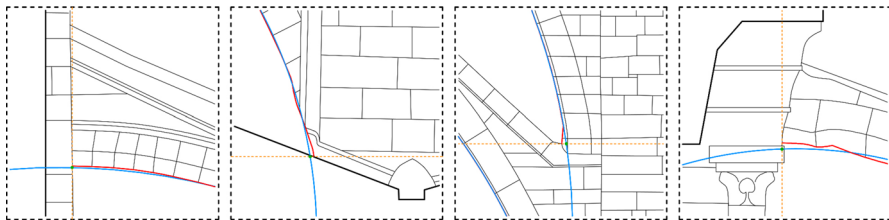


Fig. 5 Detailed view of the end points on edges \mathcal{B}_1 , \mathcal{B}_4 , \mathcal{B}_5 and \mathcal{B}_{10} . The end point of each arc on the regression circle is shown in green. The horizontal and vertical straight lines passing through the end points (topmost end point and lowermost end point) are shown in orange and with a dotted line

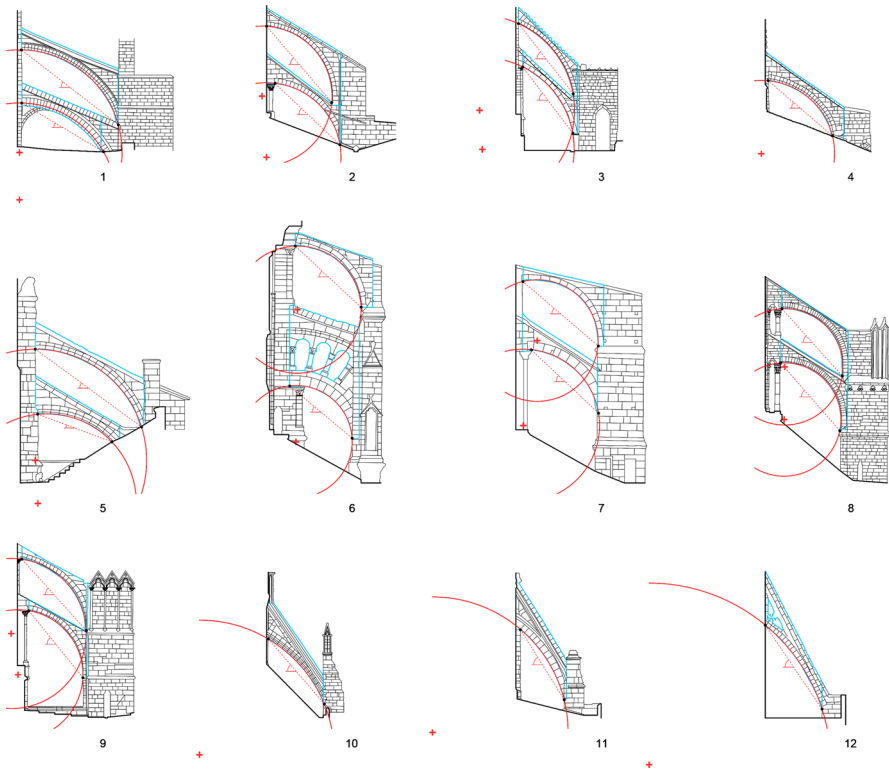


Fig. 6 Graphic results for the circular regression calculation of the flyer lower edges B_{1-20} . The flying buttress numbering is the same as in Fig. 4. The regression circle arc is highlighted with a red line, and the circle center O is marked with a red cross. The inclination α of each flyer is shown with a red dotted line. The regions R_{1-20} considered in “Objective Procedure to Determine the Inclination of a Flying Buttress Arch Using Mechanical Criteria and Graphic Statics Techniques” are highlighted in blue

in specialized literature (Heyman 1969, 1995; Moya 2011). Nonetheless, we want to make clear that, in order to determine the lines of maximum and minimum thrust for each flyer arch, we have based our work on the analysis by Ungewitter and Mohrmann (1890), taking into account the following:

- The voussoirs of the flyer arch have an unlimited resistance to compression.
- The thrusts on the flyer arch are mainly horizontal.

The line of maximum thrust, shown in orange in Fig. 7, originates at the lower third of the left vertical boundary of the flyer arch, and ends at the upper third of the right vertical boundary of the flyer arch. The line of minimum thrust, shown in green in Fig. 7, originates at the upper third of the left vertical boundary of the flyer arch, and ends at the lower third of the right vertical boundary of the flyer arch (Fig. 7).

Table 2 Angle values of inclination α , β and γ (according to the classical, mechanical and geometric criterion, respectively) of all the flyer arches considered in this paper

Cathedral	Arch position	Edge	Region	r	α	β	γ
Mallorca	Upper	B_1	R_1	9.60	35.6°	31.5°	29.9°
	Lower	B_2	R_2	9.05	30.8°	27.2°	26.2°
Burgos	Upper	B_3	R_3	6.54	49.5°	39.6°	42.8°
	Lower	B_4	R_4	6.96	45.2°	41.5°	36.4°
León	Upper	B_5	R_5	8.89	52.2°	49.7°	49.1°
	Lower	B_6	R_6	8.58	52.9°	47.9°	48.4°
Oviedo		B_7	R_7	6.86	39.3°	36.1°	38.2°
Toledo	Upper	B_8	R_8	10.4	35.4°	32.1°	31.7°
	Lower	B_9	R_9	8.39	20.1°	23.3°	25.4°
Chartres	Upper	B_{10}	R_{10}	5.95	42.1°	29.5°	34.7°
	Lower	B_{11}	R_{11}	5.25	47.8°	29.1°	32.3°
Saint Pierre in Chartres	Upper	B_{12}	R_{12}	5.68	38.6°	27.6°	29.5°
	Lower	B_{13}	R_{13}	7.12	39.9°	37.8°	33.8°
Amiens	Upper	B_{14}	R_{14}	5.44	38.1°	40.2°	41.3°
	Lower	B_{15}	R_{15}	5.31	45.3°	37.5°	39.7°
Saint Denis	Upper	B_{16}	R_{16}	7.03	43.8°	42.4°	39.1°
	Lower	B_{17}	R_{17}	6.07	49.2°	42.4°	41.8°
Salisbury		B_{18}	R_{18}	12.60	48.8°	50.9°	50.5°
Wells		B_{19}	R_{19}	12.67	58.2°	55.3°	56.7°
Bath		B_{20}	R_{20}	16.98	55.9°	58.2°	59.5°

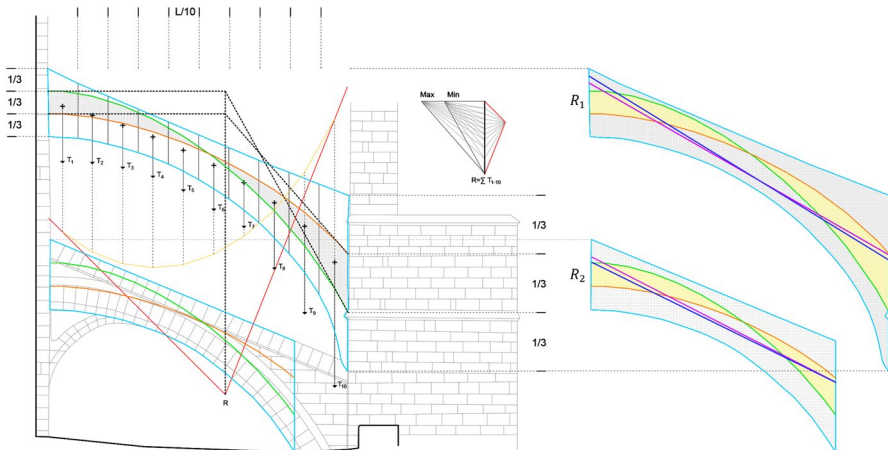


Fig. 7 Results of applying the graphic statics techniques to region R_1 (upper flyer) and region R_2 (lower flyer) of the flying buttress from Mallorca cathedral. The minimum thrust line is shown in green. The maximum thrust line is shown in orange. The maximum and minimum thrust lines delimit the point clouds I_1 and I_2 , which are highlighted in yellow. The regression lines ρ_1 and ρ_2 for clouds I_1 and I_2 are shown in dark blue. The regression lines σ_1 and σ_2 for the entire point clouds contained in region R_1 and region R_2 of the flying buttress are shown in purple

Figures 8 and 9 show the maximum and minimum thrust lines for the 20 regions R_j considered in this paper. Next, for each flyer, we define a homogeneous point cloud I_j which is delimited by the two thrust lines and the vertical boundaries of the corresponding region. As an example, the cloud points I_1 and I_2 are highlighted in yellow in Fig. 7. Once this cloud point I_j has been determined, its regression line ρ_j can be calculated and drawn. The inclination β_j of this regression line is what we are proposing as inclination of the flyer arch, since it takes into account its entire geometry and mechanical function. The regression line ρ_j for the point cloud I_j of each flyer arch is shown in dark blue in Figs. 8 and 9. The inclination values β_j of these regression lines are shown in Table 2. “Results” contains some brief comments on the results obtained.

Figures 8 and 9 show the results obtained with the previously described graphic statics techniques. In order to validate the maximum and minimum thrust lines, each flyer was analyzed using the finite element method (Oñate 1995). The software Autodesk Robot Structural Analysis Professional was used for this analysis. For these models, each flyer arch was considered to be a shell type element having constant thickness. The shell element was meshed into finite elements having three and four nodes. A 30×30 cm mesh was used; a denser

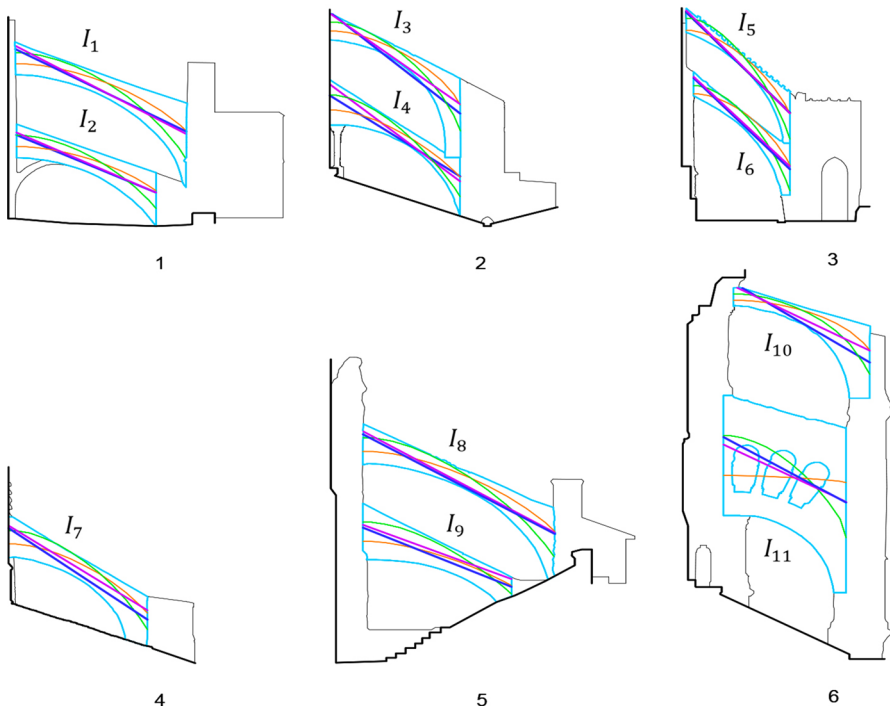


Fig.8 Results of applying the graphic statics techniques to the regions I_{1-11} of the flyer arches considered in this paper. The same colours have been used as for the specific case shown in Fig. 7, and the same numbering as in Figs. 4 and 6

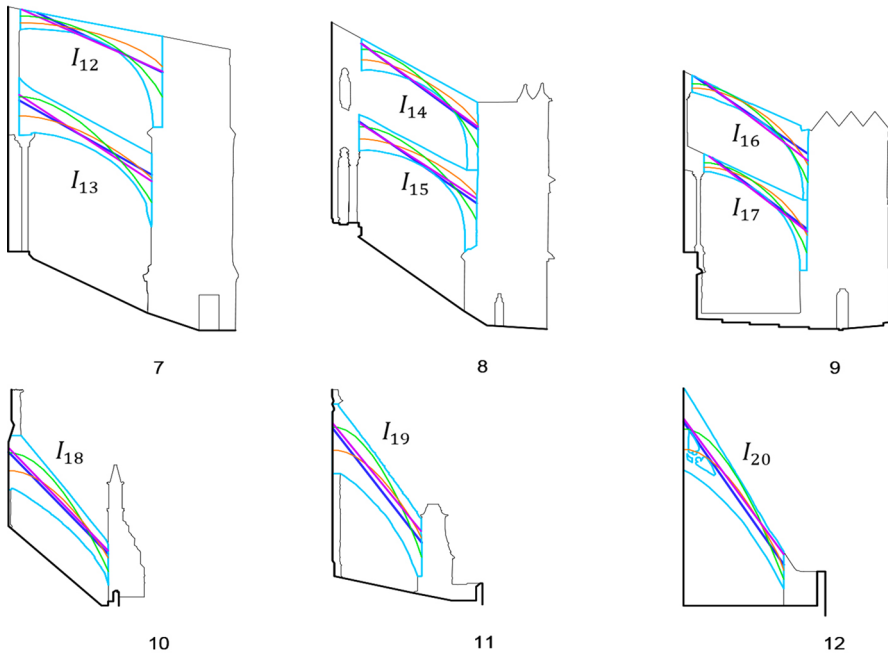


Fig.9 Results of applying the graphic statics techniques to the regions I_{12-20} of the flyer arches considered in this paper. The same colours have been used as for the specific case shown in Fig. 7, and the same numbering as in Figs. 4 and 6

mesh was used for regions with a more complex geometry. The stones used in the arches were considered as a set of elastic elements which are separated by potential fracture lines (López et al. 1998). Thus, using a non-linear process of consecutive analyses, successive discontinuities between elements were introduced until a “fractured” model was obtained. In the previous model there were traction forces, but in this fractured model, equilibrium is only reached with compression forces. The number of necessary approximations was higher for the flying buttresses which present more irregularities. The vertical boundaries of the flyer were defined as supports. The vertical displacement is conditioned by the stiffness of the support, which varies depending on the height. This stiffness variation is equivalent to the axial stiffness variation of the buttress along the vertical boundary of the flyer.

Figures 10 and 11 show the isostatic lines obtained for the model of forces. These lines represent the direction field of the compression forces in each flyer arch.

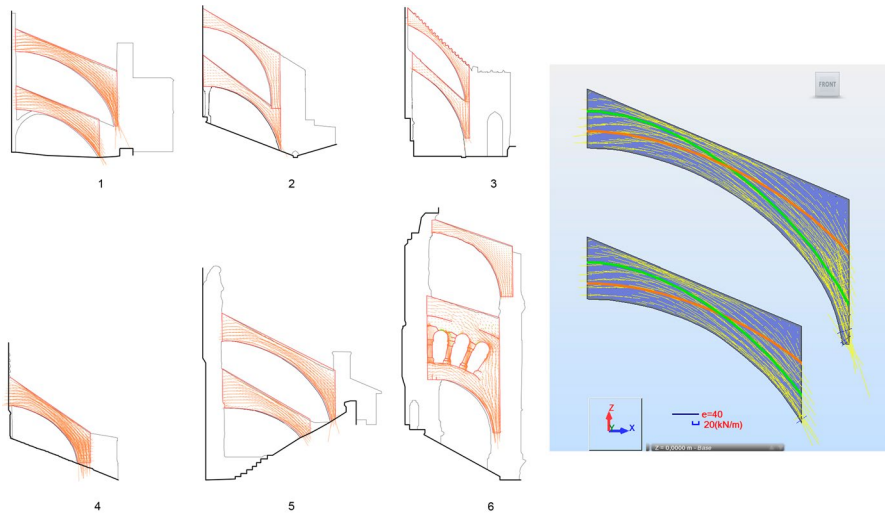


Fig. 10 Graphic results of applying the finite elements method to the flyer arches of the first six flying buttresses considered in this paper. On the right, detailed view of the flyer arches from the flying buttress from Mallorca cathedral. The isostatic lines calculated with the software Autodesk Robot Structural Analysis Professional are shown in yellow. The maximum thrust line is shown in orange. The minimum thrust line is shown in green

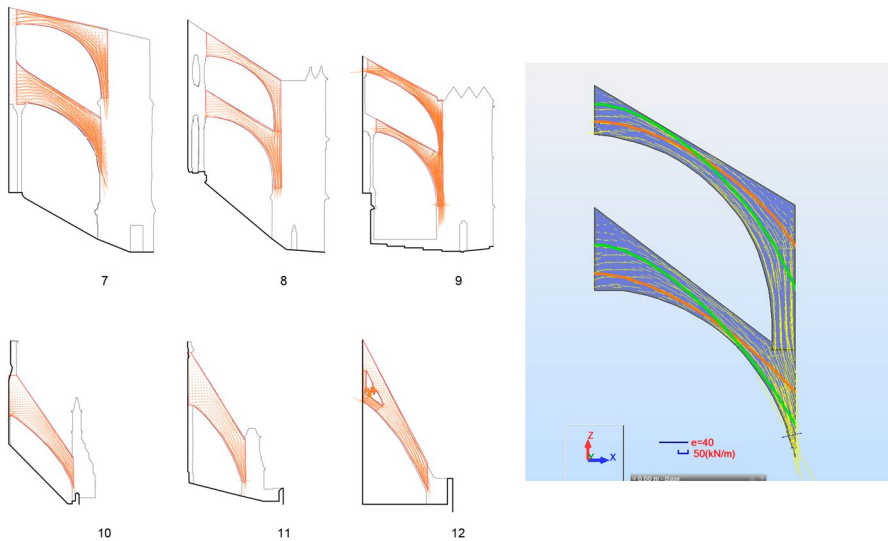


Fig. 11 Graphic results of applying the finite elements method to the flyer arches of the last six flying buttresses considered in this paper. On the right, detailed view of the model created for the flyer arches of the flying buttress from Burgos cathedral. The same colours have been used as for the specific case shown in Fig. 10

Results

Table 2 shows the numerical results obtained by the authors.

Geometric Approximation of the Newly Proposed Inclination β

The newly proposed method to determine a flyer inclination β requires the knowledge and the calculations previously described in “Objective Procedure to Determine the Inclination of a Flying Buttress Arch Using Mechanical Criteria and Graphic Statics Techniques”. Nonetheless, there may be some people who are interested in using this new method to calculate the flyer inclination but, for whatever reason, cannot or do not wish to make the necessary calculations. Taking this into account, we describe a purely geometric method which requires much simpler calculations. The inclination value γ determined with this method is a geometric approximation of the value β .

This approximation process consists in determining the inclination γ_j of the regression line σ_j for the entire study object, in other words, for region R_j . Figures 7, 8 and 9 show this regression line in purple.

Of course, the regression line σ is much simpler to calculate than the regression line ρ . The value β can be used as an approximation of the value γ , but it is the user who, depending on his accuracy requirements, should decide which of both regression lines (σ or ρ) he or she needs to calculate.

Readers familiar with the software product Rhinoceros can use the tool “FitPoints” to determine the regression circle which best fits a point cloud.

Figure 12 shows in detail the inclinations γ_{5-6} , γ_{14-15} and γ_{19} . Figures 8 and 9 show all the regression lines σ_j . Figure 7 shows line σ_1 and line σ_2 in greater detail. Table 2 shows the numeric values of all inclinations γ_j .

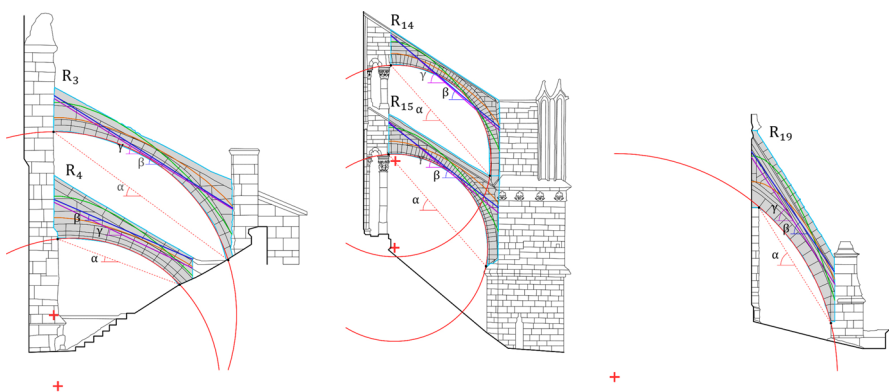


Fig. 12 Some graphic results. On the left, inclinations α , β and γ (R_3 : 49.5°, 39.6°, 42.8°; R_4 : 45.2°, 41.5°, 36.4°) of the two flyers that make up the flying buttress from Burgos Cathedral. In the center, inclinations α , β and γ (R_{14} : 38.1°, 40.2°, 41.3°; R_{15} : 45.3°, 37.6°, 39.7°) of the two flyers that make up the flying buttress from Amiens Cathedral. On the right, inclinations α , β and γ (R_{19} : 58.2°, 55.3°, 56.7°) of the flyer arch from Wells Cathedral

Table 3 Statistical parameters obtained from the angle values shown in Table 2

Statistical parameters	β	γ
Mean	39.3°	38.9°
Standard deviation	9.36	9.54
Pearson's coefficient of variation cv	0.238	0.245
Covariance $\beta\gamma$	86.226	
Pearson's correlation coefficient $cr\beta\gamma$	0.965	
Squared Pearson's correlation coefficient $\beta\gamma$	0.931	
Student's t test value	0.999	
Significance level	3×10^{-12}	
Relative error between means	0.87%	

γ as an Approximation to β

In order to statistically determine if γ is an approximation of β , the following steps are taken. First, we calculate whether or not there is a strong linear correlation between sets β_j and γ_j of inclination values (see Table 2). We find that Pearson's correlation coefficient is 0.96. Applying Student's t-test, the probability of non-correlation is 3×10^{-12} . Nonetheless, that is not sufficient to show a statistical similarity between the value pairs β_j and γ_j . Therefore, we check to see if the means of both sets differ by a small relative error, and we find that this error is only 0.87%. We also check if both means are representative of their respective sets of inclination values, and we find that their Pearson's coefficients of variation are 23.8 and 24.4%, respectively. Combining all results, we can claim that, from a statistical point of view, the inclination γ is an approximation of the inclination β .

As a reminder, Pearson's coefficient of variation cv is $\frac{s}{m}$, where s is the standard deviation, and m is the mean. The mean m is usually considered to be representative of its set if cv is less than 25%. Pearson's correlation coefficient cr is $\frac{s_{\beta\gamma}}{s_{\beta}s_{\gamma}}$, where s_{β} is the standard deviation of the set of values β_j , s_{γ} is the standard deviation of the set of values γ_j , and $s_{\beta\gamma}$ is the covariance of both sets. If Student's t-test with $n - 2$ degrees of freedom ($n = 20$ in our case) is applied, the parameter $P_{\beta\gamma}$ is found such that the hypothesis of non-correlation is rejected with a probability (significance level) of $1 - P_{\beta\gamma}$. A significance level under 0.01 is considered to be very good.

After making the relevant calculations, we obtain the values which are summarised in Table 3.

Acknowledgements In order to carry out this research, we needed to access all the flying buttress considered in our analysis. We wish to thank the following people and entities for making this possible: The Cathedral Chapter and Mrs Catalina Mas, Director of Mallorca Cathedral's Archive; Mr Víctor Ochotorena, churchwarden of Burgos cathedral; Mr Antonio Trobajo, Dean of Burgos Cathedral; Mr César García, historian of Oviedo Cathedral; Mr Isidoro Castañeda, Director of Toledo Primate Cathedral's archive and chapter library; Mr Gilles Fresson, Attaché de coordination of Chartres Cathedral and Saint Pierre church in Chartres; Mr Eric Charlet, Technicien des services culturels et des bâtiments de France, and Mr Antoine Paoletti, architecte des bâtiments de France et conservateur of Amiens

Cathedral; Mr François-Xavier Créteaux, ingénieur des Services Culturels et du Patrimoine of Saint Denis Cathedral; Mr Gary Price, Clerk of the works of Salisbury Cathedral; Mr Jez Fry, Clerk of the works of Wells Cathedral; and lastly, Mrs Sarah Fielding, Head of visitors experience in Bath Cathedral.

All images are by the authors.

Funding Open access funding provided by Universitat Rovira i Virgili.

Open Access This article is licensed under a Creative Commons Attribution 4.0 International License, which permits use, sharing, adaptation, distribution and reproduction in any medium or format, as long as you give appropriate credit to the original author(s) and the source, provide a link to the Creative Commons licence, and indicate if changes were made. The images or other third party material in this article are included in the article's Creative Commons licence, unless indicated otherwise in a credit line to the material. If material is not included in the article's Creative Commons licence and your intended use is not permitted by statutory regulation or exceeds the permitted use, you will need to obtain permission directly from the copyright holder. To view a copy of this licence, visit <http://creativecommons.org/licenses/by/4.0/>.

References

- Blas Orive, Antonio de. 2019. *El puntal de piedra, estática y estética del arbotante gótico*. Madrid: Universidad Politécnica de Madrid.
- Choisy, Auguste. 1899. *Histoire de l'architecture Tome II*. Paris: G. Beranger.
- Henriet, Jacques. 1978. Recherches sur les premiers arc-boutants. Un jalon: Saint-Martin-d'Etampes. *Bulletin monumental* 136: 309-323.
- Henriet, Jacques. 1982. La cathedrale Saint-Etienne de Sens: Le parti du premier maître et ses campagnes du XIIIe siècle. *Bulletin monumental* 140: 152-212.
- Heyman, Jacques. 1969. The safety of masonry arches. *International Journal of Mechanical Science* 11: 363-385.
- Heyman, Jacques. 1995. *The stone skeleton: Structural engineering of masonry architecture*. Cambridge: Cambridge University Press.
- Lefevre-Pontalis, Eugene. 1919. Etude historique et archiologique sur l'eglise de Saint-Germain-des-Pris. *Congrès archiologique* 82: 363.
- López, Javier, Sergio Oller, Eugenio Oñate. 1998. *Cálculo del comportamiento de la mampostería mediante elementos finitos*. Barcelona: CIMNE.
- Moya, Diego. 2011. El origen de los arbotantes en la historia de la Arquitectura. En el X Certamen Arquímides de Introducción a la Investigación Científica. Ministerio de Educación y Consejo Superior de Investigaciones Científicas.
- Nikolinakou, Maria K., Andrew J. Tallon and John A. Ochsendorf. 2005. Structure and form of early Gothic flying buttresses. *Revue Européenne de Génie Civil* 9(9-10): 1191-1217.
- Oñate, Eugenio. 1995. *Cálculo de estructuras por el método de elementos finitos. Análisis estático lineal*. Barcelona: CIMNE.
- Prache, Anne. 1976. Les arcs-boutants au XIIIe siècle. *Gesta* 15: 37.
- Stanley, David J. 2006. The Original Buttressing of Abbot Suger's Chevet at the Abbey of Saint-Denis. *Journal of the Society of Architectural Historians* 65: 353.
- Ungewitter, Georg G., and Karl Mohrmann. 1890. *Lehrbuch der Gotischen Konstruktionen*. Leipzig: Weigel Nachfolger.
- Viollet-Le-Duc, Eugène. 1996. *La construcción medieval*. Madrid: Instituto Juan Herrera.

Publisher's Note Springer Nature remains neutral with regard to jurisdictional claims in published maps and institutional affiliations.

Albert Samper is an architect who obtained his Ph.D. in Architecture at the University of Rovira i Virgili in 2014. Presently, he is an assistant professor of architecture at the same university and his main fields

of interest are: architectural heritage, architectural representation and the application of geometry to architecture.

Rodrigo Martín-Sáiz is an architect who obtained his Ph.D. in Architecture at the Polytechnic University of Catalonia in 2015. Presently, he is an adjunct professor of architecture at the University of Rovira i Virgili and his main field of interest is the analysis of architectural structures.

Blas Herrera is a geometer who obtained his Sc.D. in Mathematics at the University Autònoma of Barcelona in 1994. Presently, he is a full professor of applied mathematics at the University Rovira i Virgili of Tarragona. His main fields of research interest are classical and differential geometry, and the application of geometry to architecture and engineering.